

6-C

Fusion Neutron Test Facility Requirements for Interactive Effects in Structural and High-Heat-Flux Components

N. M. Ghoniem¹ and J. B. Whitley²

A relevant design data base is needed for structural components in near-term and commercial fusion devices. A high-flux, high-fluence fusion neutron test facility is required for testing the failure mechanisms and lifetime-limiting features for first wall, blanket, and high-heat-flux components. We describe here the key aspects of the fusion environment which influence the response of structural and high-heat-flux components. In addition to test capabilities for fundamental radiation-effects phenomena, e.g., swelling, creep, embrittlement, and hardening, it is shown that the facility must provide an adequate range of conditions for accelerated tests to study the limitations on component lifetime due to the interaction between such fundamental phenomena. In high-heat-flux components, testing of the failure mechanisms of duplex structures is shown to require maintenance of an appropriate temperature gradient in the 14-MeV neutron field. Thermal stresses are shown to result in component failure, particularly when the degradation in the thermal conductivity and mechanical properties by irradiation are considered. Several factors are discussed for assessment of the failure modes of the first wall and blanket structures. These are displacement-damage dose and dose rate, the amount of helium gas generated, the magnitude of irradiation and thermal creep, prototypical temperature and temperature-gradient distributions, module geometry, and external mechanical constraints.

KEY WORDS: 14-MeV neutrons; fusion materials test facility; interactive effects; structural and high-heat-flux components.

1. INTRODUCTION

Optimal design of first wall (FW), blanket (B), and high-heat-flux (HHF) components in fusion devices requires extensive knowledge of the performance of these components in their anticipated environment. Successful commercial operation of fusion devices is critically dependent upon the development of materials and components for safe and economical operation. Failure to achieve this important goal is

apt to jeopardize commercialization of fusion energy, even when scientific demonstration of adequate net energy production is achieved. It is well accepted now that materials and component performance are important ingredients in the development of economically- and environmentally-competitive fusion energy sources.

Many features of materials performance have been successfully studied by a combination of available experimental and theoretical techniques. Novel alloys and components have been developed in the U.S., Japan, and Europe for fusion applications. Fortunately, many alloy systems were studied with the aid of existing neutron test facilities. Fission reactors

¹School of Engineering and Applied Science, University of California at Los Angeles, Los Angeles, California 90024.

²Sandia National Laboratories, Albuquerque, New Mexico 87185.

76

provide the necessary volume and fluence for radiation-effects tests while low-fluence, 14-MeV neutron facilities, e.g., RTNS-II, FNS, etc., provide experimental tools for investigating basic aspects of 14-MeV neutron interactions with alloys. High-energy ion-beam facilities are used to screen alloy systems for their radiation sensitivity and to develop new alloys which are highly resistant to the damaging effects of neutrons. The approach is quite logical, since an alloy which deteriorates very quickly in a fission or ion-beam environment will most likely do the same, or even worse, under fusion conditions. Likewise, plasma-facing components are tested under thermal conditions which simulate their anticipated operation. Failure of these components in the simulated thermal environment will inevitably guarantee their failure, perhaps under even less severe thermal conditions, when they are tested in a prototypical fusion environment. Information which is more reliable will be obtained if thermomechanical tests are performed on irradiated components. One must note that no significant information on the interactive modes of failure is obtained when the tests are *sequential*.

Obviously, the most direct method for development and optimization of structural and HHF components is to perform tests in the real environment for which they are designed. However, the attainment of such an environment requires successful operation of the very particular fusion device which we design. A solution to this inconsistent logic is to devise a hierarchical strategy which combines theory, experiment, and design methodology as illustrated in Fig. 1. This strategy has already been implemented, at least partially, with fruitful results for alloy and component development. One may still ask why there is a need for a dedicated 14-MeV neutron test facility. In fact, it is natural to wonder about how critical the need is for information obtained from such a test facility. It is our purpose in this article to demonstrate that a fusion-materials test facility is not only necessary, but it must also be designed to provide adequate information on interactive failure modes in the fusion environment. Without this type of information, the gap between present-day experimental information and required design data may be so large as to render future designs highly unreliable. A facility which can supply this information will indeed be a cornerstone in the strategy logic for successful and optimized component design.

First wall (FW) and blanket (B) components are expected to operate with an FW neutron wall loading in the range 0.5–10 MW/m². The displacement dam-

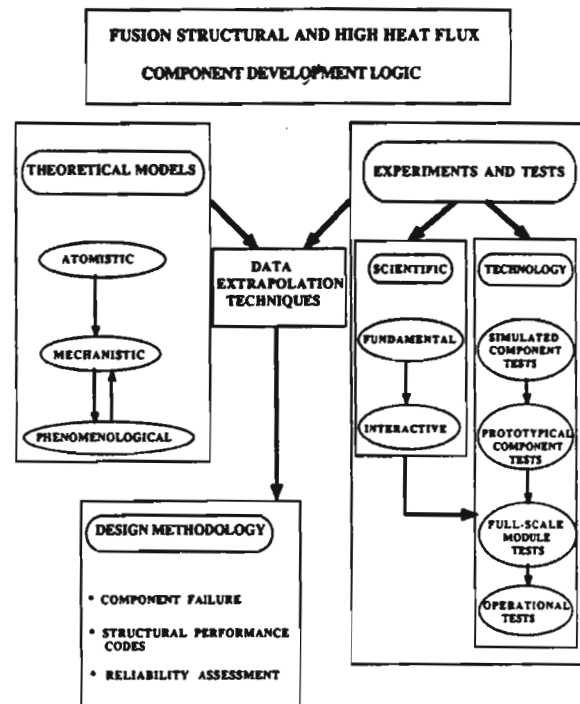


Fig. 1. Fusion structural and HHF component development logic.

age, helium production, and volumetric heating rates are dependent upon the structural alloy and vary considerably with distance away from the FW toward the magnets. A surface heat flux of 0.1–3 MW/m² is also expected on the FW from plasma particles and radiation. Helium generation is material and component dependent and can vary by orders of magnitude. Since damage and heating parameters are dependent on the specific design, material, and location within the FW/B system, one must identify ranges of conditions for critical tests to ensure overall reliable operation of FW/B modules.

The interiors of magnetically-confined fusion devices are lined with many components that receive high particle and heat fluxes. These components include limiters, divertor plates, wall armor, and rf launchers. They interact directly with the plasma and hence must not unduly contaminate or otherwise degrade the plasma performance. This close coupling to the plasma performance, along with the severe environment to which they are exposed, makes their reliable and consistent performance a major design issue (see Refs. 1–8). Typical heat-flux levels for these components vary from 1–30 MW/m² during normal operation, while plasma disruptions may deliver energy densities of 5–20 MJ/m² during times of

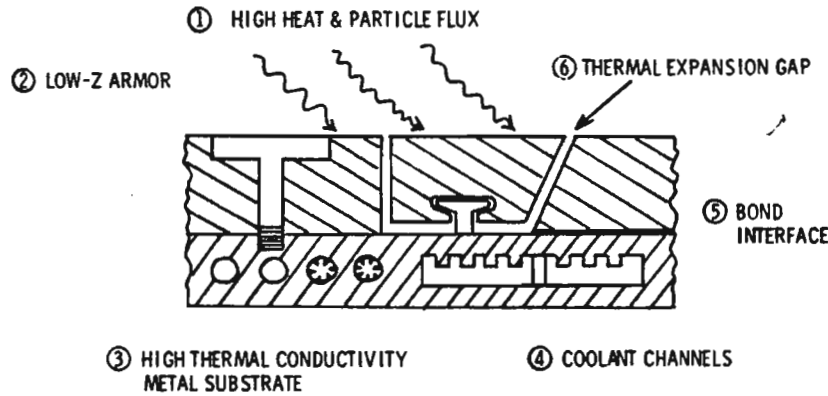


Fig. 2. Schematic representation of a generic limiter design.

0.1–10 ms. Runaway electrons of energies greater than 100 MeV may also strike the components, and they will be exposed to a basically uncollided 14-MeV neutron flux. Plasma erosion by sputtering may be the life-limiting factor and could require frequent change-out of high-particle-flux components as often as every few weeks. Thermal effects such as thermal fatigue and thermal shock resistance are also critical concerns.

The design of HHF components for the fusion environment is one of balancing the many different, often conflicting, materials requirements to obtain the optimum solution. For example, the plasma surface material is usually required to be a low atomic-number material, such as carbon or beryllium, to reduce plasma radiation losses and to avoid dilution

effects from impurities introduced by sputtering.⁽⁹⁾ These low atomic-number elements are usually not good structural materials, however, and are not compatible with the water or helium coolant required to remove the incident power flux. For these reasons, these designs for future long-pulse devices are usually duplex structures with an actively cooled substrate or a material with a high thermal conductivity, e.g., copper alloy, with a plasma-facing armor of carbon, beryllium, or some other material applied using, for example, brazing for carbon or plasma spray for beryllium. A schematic representation of some of these design options is shown in Fig. 2.

As an example, Fig. 3 shows a finite-element thermal analysis from a typical operating load. Here, a copper alloy substrate is cooled using high velocity

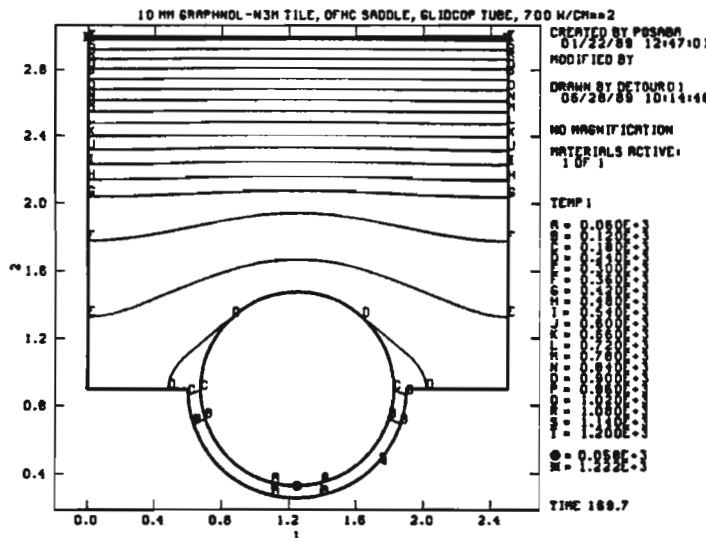


Fig. 3. Temperature distributions for C/Cu water-cooled limiter.

water and is armored using 10-mm thick graphite tiles which are brazed to the surface. A normal pulse heat load of 7 MW/m² is delivered for 1000 seconds, leading to a steady-state surface temperature of 1200°C and a temperature gradient of 1000°C across the structure. During "routine" operation, it is expected that the plasma will disrupt once in about every 100 normal pulses. This disruption will deliver an energy burst of 10 MJ/m² in about 0.1 ms, accompanied by a large mechanical shock produced by induced eddy current. During this disruptive pulse, the component will be in a neutron flux field of 10¹⁴–10¹⁵ cm²/s.

In this article, we present a discussion of the current state of knowledge regarding the anticipated performance of structural (FW/B) and HHF components in commercial fusion devices. From this vantage point, we establish the required characteristics of a dedicated fusion-materials test facility. Our objective is to delineate the features that will result in a high probability of success for the design of commercial fusion devices. In Section 2, a presentation of testing requirements for structural components is given. In Section 3, we analyze specific requirements for HHF components and give our conclusions and recommendations in Section 4.

2. TESTING REQUIREMENTS FOR STRUCTURAL COMPONENTS

The ultimate goal of radiation-effects testing of structural components is to determine their qualifications for use in the design of safe, reliable, and economical components. We must differentiate, however, between fundamental radiation-response tests and interactive radiation-effects tests. Fundamental radiation-response experiments are designed to determine the dependence of fundamental phenomena, e.g., swelling, creep, and embrittlement, on material and irradiation variables, e.g., alloy composition, fabrication, metallurgical variables, temperature, fluence, flux, gas content, and bombarding particle energy. Significant progress has been made in exploring this extensive range of variables, although uncertainties still exist regarding the effects of the specific fusion environment. The current data base still does not allow a reliable prediction of these fundamental phenomena in the fusion environment. A fusion-materials test facility with modest demands on fluence and volume will most certainly increase the

reliability of our predictions of the fundamental phenomena.

Theoretical models are essential for planning new experiments and for understanding the mechanisms involved in both fundamental and interactive experiments. Atomistic models are based on basic interatomic potentials and on the physics of radiation interaction with matter. Mechanistic models describe the rate processes of point-defect-microstructure interaction, and provide a basis for describing microstructure evolution under irradiation. Phenomenological models are more appropriate for the description of complex changes in the physical and mechanical properties of materials in the fusion environment, and are closely related to experimental observations. A balanced theoretical program combines these four elements and provides a basis for experimental planning as well as for data extrapolation. In this section, we will focus on the testing requirements for *interactive* phenomena only. Requirements for experiments on fundamental phenomena are discussed by Ishino *et al.*⁽¹⁰⁾

Early predictions of the end-of-life (EOL) for FW/B components were based on independent limits on swelling (2%–10%) and reduction in the total elongation (0.5%–2%).⁽¹¹⁾ It has been recognized by the research community that failure of FW/B components may occur because of a number of competing mechanisms.^(12–14) Harkness and Cramer⁽⁴⁾ identified three criteria which could be used to determine the EOL for FW/B components. The first includes processes which result in coolant leakage (leak-before-break) or catastrophic component failure. Crack propagation by creep or fatigue through the FW/B walls is a prime example. The second criterion is based on a maximum limit of dimensional deformation induced by swelling or creep. This limit is design dependent and is determined by considerations of maintenance and planned operation. The third category comprises deformation limits, particularly at high temperatures, so that unspecified failure modes do not occur. This limit is set by experience and is usually considered as a few percent change in the linear strains. The high-temperature creep-strain limit is based on this criterion, and is closely related to the amount of ductility retained in the material. For example, at high temperature, helium gas enhances grain-boundary fracture by cavitation, thus lowering the allowable stress.

Detailed work on structural analyses of FW/B components, including radiation effects, has been

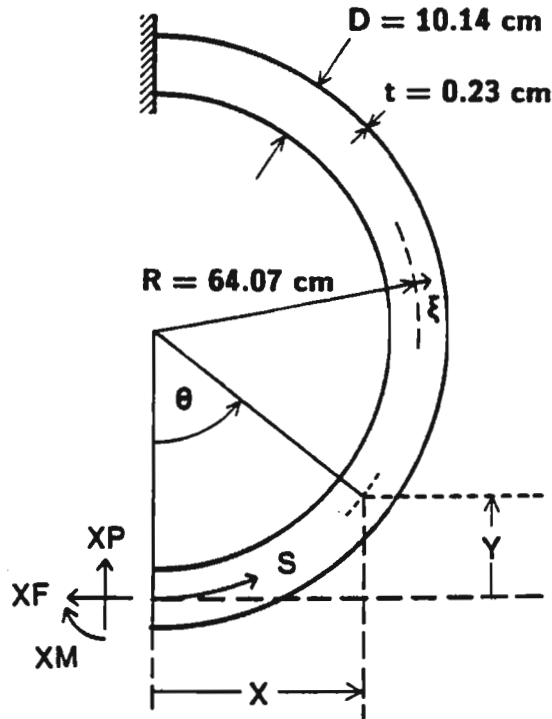


Fig. 4. Configuration of a representative FW curved pipe.

fairly limited.⁽¹⁵⁻¹⁹⁾ However, several important features of failure by fatigue-crack propagation have been addressed.⁽⁴⁾ Since then, a recognition of the importance of steady-state operation for long component lifetime was realized. In the following, we present results of an inelastic stress-analysis model to illustrate the complex nature of interactive radiation-induced phenomena.

2.1. Structural Model

In a number of recent fusion reactor designs, pipes have been considered as FW elements.^(20,21) We will consider a representative curved pipe as our FW model (the configuration is shown in Fig. 4). Furthermore an extension of classical beam theory will be used to reduce the computational burden and will include the following irradiation strains: (1) thermal strain due to thermal expansion, (2) swelling strain, (3) irradiation creep strain, and (4) thermal creep strain. In Fig. 4, the unknown end reactions (XM, XF, and XP) result from the inelastic strains. Because the tube is curved and statically indeterminate, we must consider the axial, radial, and rotational modes of deformation. These deformation

modes result from nonlinear variations of the inelastic strains over the pipe. Using virtual work principles, the flexibility matrix $\underline{\underline{F}}$ can be obtained. It gives the deflections at the free end of a singly clamped beam resulting from unit loads at that end. For our pipe model, we can easily obtain:

$$\underline{\underline{F}} = \frac{R^3}{EI} \begin{pmatrix} \pi & \pi & 2 \\ \pi & 3\pi/2 & 2 \\ 2 & 2 & \pi/2 \end{pmatrix} \quad (1)$$

where the first row gives the rotations resulting from unit moment, unit axial force, and unit radial force, respectively. Similarly, the second and third rows give the axial deflections and the radial deflections, respectively. The modulus of elasticity is E , I is the moment of inertia, and R is the major radius of the pipe. If the unknown end reactions are assembled into the vector \underline{X} , the end deflexives are $\underline{\underline{F}}\underline{X}$. Let us denote the deflections induced by the four sources of inelastic strains outlined above as \underline{S} , where

$$\underline{S} = - \begin{pmatrix} R \int w' ds \\ \int w' y ds - \int \bar{e}' \cos \theta ds \\ \int w' x ds - \int \bar{e}' \sin \theta ds \end{pmatrix} \quad (2)$$

w' is the change in curvature resulting from inelastic strains and \bar{e}' is the average inelastic strain at any given cross section.

$$\bar{e}' = \frac{1}{A} \int \left(\alpha T + \frac{\Delta v}{3v} + e_{irr}^c + e_{th}^c \right) dA \quad (3)$$

where αT is the thermal strain, $\Delta v/3v$ is the linear swelling strain, e_{irr}^c is the irradiation creep strain, and e_{th}^c is the thermal creep strain. A deflection equation for the end rotations and axial and radial deflections can be written as:

$$\underline{\underline{F}}\underline{X} + \underline{S} = \underline{D}, \quad (4)$$

where \underline{D} is generally determined by the boundary conditions. The unknown end reactions are obtained by inverting Eq. (4) once the components of \underline{S} are determined. The resultant forces and moment acting on any cross section of the pipe can be easily calculated from the vector \underline{X} of end reactions. The axial

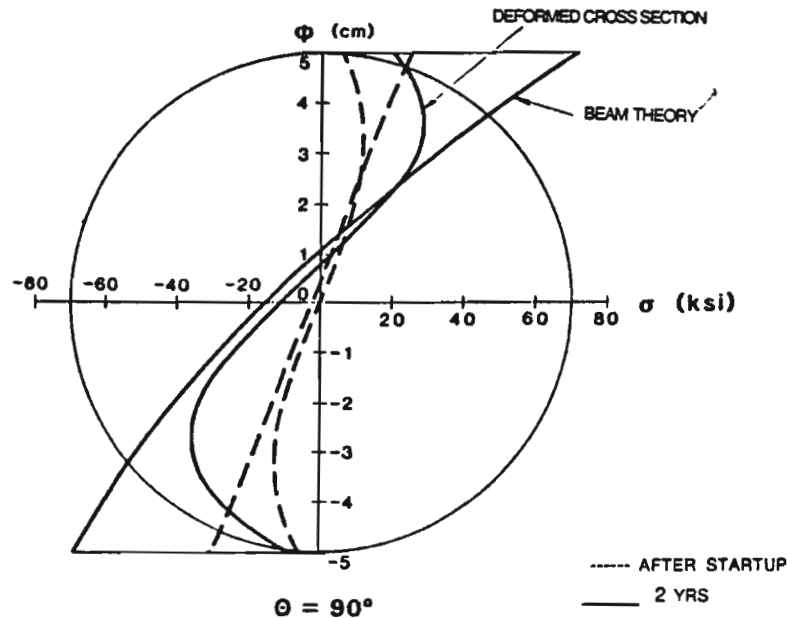


Fig. 5. Stress distributions over the pipe's cross section, with and without cross-section deformation.

force, f , can be used to calculate the axial stress

$$\sigma = \frac{f}{A} - E(e' - \bar{e}') + \xi(1 - K_I \xi^2) \left(\frac{M}{K_{III}} - Ew' \right) \quad (5)$$

where ξ is the displacement away from the neutral axis, M is the moment at the cross section, and K_I and K_{III} are constants. The pipe's deflection at any angle θ is obtained by applying Eq. (4) at the desired angle.

We now apply Eqs. (1)–(5) on a martensitic steel pipe, with the properties of HT-9. The constitutive equations for swelling, irradiation, and thermal creep strains are those of Ref. 22. The thermal field is assumed to be linear in both θ and ξ :

$$T(\theta, \xi) = T_{out} + \left(\frac{T_{in} - T_{out}}{\pi} \right) \theta + \frac{\xi \Delta}{2r} \quad (6)$$

where T_{in} and T_{out} are inlet and outlet pipe temperatures, respectively, and Δ is the front-to-back temperature drop of the pipe.

Figure 5 shows a comparison between standard beam theory and the present analysis. Instead of the traditional linear stress distribution over the cross section, our analysis shows that the stress distribution in a curved pipe is nearly parabolic, with the maximum occurring in an inner fiber. Figure 6 illus-

trates the significance of swelling strains if creep relaxation is not accounted for. The maximum stress in the pipe increases by a factor of eight over the thermal stress after 2 years of operation at 69 dpa/yr (displacement per atom/year). No translation of this pipe's ends were allowed in these calculations, although specified end translations can mitigate some of the accumulated swelling stress.

The inclusion of irradiation creep into the analysis results in a reduction of the accumulated stress, which is calculated at $\theta = 120$ deg. One of the points which we emphasize in our analysis here is the uncertainty in the values of measured irradiation creep-strain rates, as given by the relationship:

$$\dot{\epsilon}_{irr}^c = A_c \delta \sigma \quad (7)$$

where δ is the displacement dose rate and A_c is the creep coefficient. Available data on HT-9 show a range from 7×10^{-7} to 1×10^{-5} $\text{ksi}^{-1} \text{dpa}^{-1}$. The calculated stress could be anywhere between 3–40 ksi, depending on the accuracy of the value of the creep coefficient. Since the allowable design stress of HT-9 at this location was determined to be 28 ksi, it is obviously not possible to ascertain the pipe's lifetime. Calculations which include the effects of displacement-damage gradients have shown that the maximum stress actually increases because of an overall reduction of the creep coefficient.⁽²³⁾ Damage

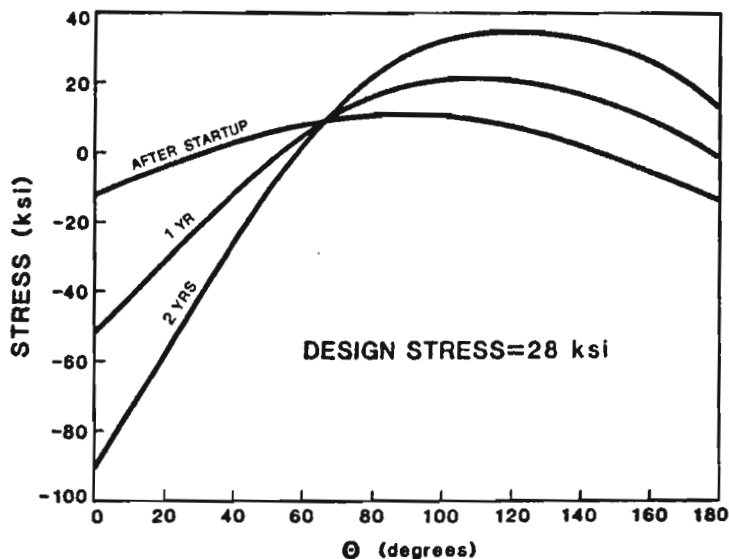


Fig. 6. Stresses along the pipe for clamped end conditions, without creep relaxation.

gradients are therefore important, and they tend to deteriorate the lifetime of FW tubes.

The effects of thermal creep are included by investigating an example where the pipe's inlet and outlet temperatures are taken as 450°C and 550°C, respectively. The effect of thermal creep on the stress distribution in the pipe is shown in Fig. 7. The stress is nonuniformly redistributed by the deformation as a result of the nonlinear stress dependence of the creep law. Although thermal creep appears to have increased the blanket lifetime by stress relaxation, the detrimental effects of increased creep strain must

be considered. The simplest criterion is to set an upper limit on the accumulated creep strain, usually 1-3%. Creep rupture by grain-boundary cavitation may be included here, but the dependence on the stress, temperature, and helium content is not well established. We conclude, therefore, that this failure mode is crudely described, and an actual determination requires self-consistent interaction between thermal creep, irradiation creep, and swelling strains.

The range of uncertainties is further illustrated by considering the pipe's lifetime as a function of the measured creep coefficient in Fig. 8. Depending on

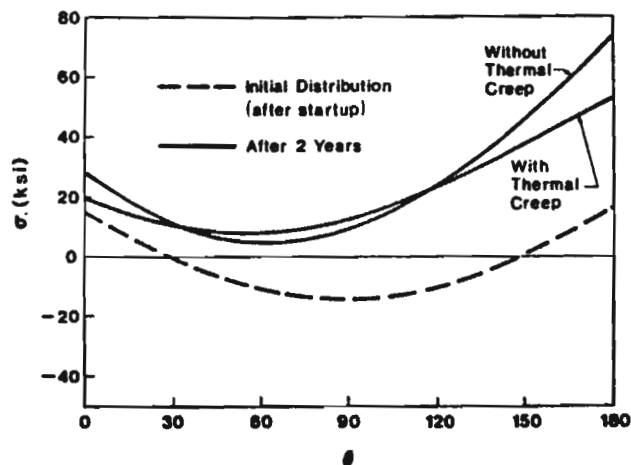


Fig. 7. Stresses along the pipe for clamped end conditions, including thermal creep.

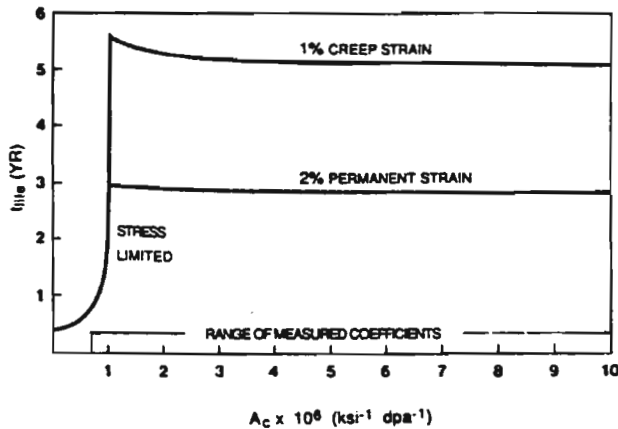


Fig. 8. End-of-life as a function of the irradiation creep coefficient.

the type of failure mode, the lifetime can range from roughly 0.5–5.5 years.

Since the uncertainty of the magnitude of the creep coefficient has a profound effect on both the nature of the failure mechanism and the corresponding lifetime, it is important to analyze the effects of uncertainties in other fundamental material properties and independent radiation-response phenomena. A probabilistic Monte Carlo method can be used for this purpose. The lifetime of the FW pipe is analyzed by coupling the deterministic approach, outlined in Eqs. (1)–(7), with probability distribution functions for the following four random variables:

1. The creep rate varies uniformly over the range $10^{-7} \text{ ksi}^{-1} \text{ dpa}^{-1} \leq z \leq 1.9 \times 10^{-5} \text{ ksi}^{-1} \text{ dpa}^{-1}$.
2. The incubation dose for swelling varies uniformly in the range $25 \leq z \leq 69 \text{ dpa}$, where z is the random variable.
3. The peak swelling rate conforms to a normal distribution with an average of $1.7\%/\text{yr}^{-1}$ and a standard deviation of 0.05%.
4. The dose rate is represented by a normal distribution with an average of $69 \text{ dpa}/\text{yr}$ and a standard deviation of $5 \text{ dpa}/\text{yr}$.

Calculations were performed with the input values sampled from the prescribed distribution functions. The objective of this exercise was to analyze the propagation of uncertainties in measurements of these independent radiation-response phenomena on the FW lifetime. The average lifetime is found to be 7.6 years, and is mainly limited by the total accumulated creep strain. Figure 9 shows the cumulative

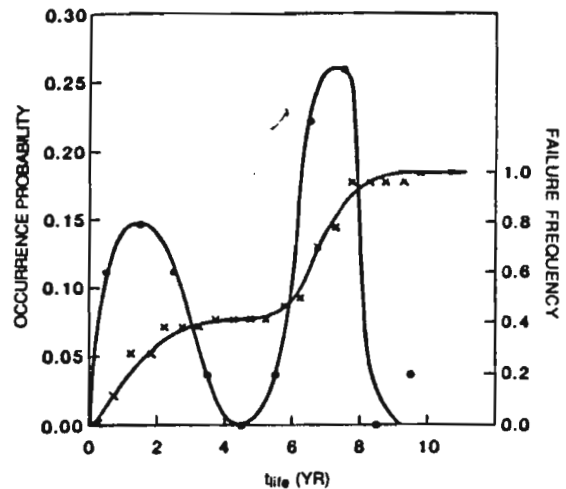


Fig. 9. Cumulative failure probability for four random variables.

failure probability and the failure occurrence frequency for the range of studied random variables. It is clearly shown that a zero failure probability of the FW component cannot be guaranteed for a lifetime of more than a few months. This is not economically tolerable. Obviously, a design which is based on the currently available data is at great safety and economic risk. The point in this example is that while radiation-effects data of fundamental phenomena seem to be reasonable as independent measurements, the interactive nature of uncertainties may well jeopardize the success of the final design.

Another source of uncertainty in independent radiation-response phenomena is that available measurements are generally taken under simplified geometrical conditions. It is well known that the stress state affects creep, fatigue, and swelling and is a function of the constraints and geometry, as we illustrate in this paper.

2.2. Testing Needs for FW/B Components

The main objective of a dedicated fusion-materials test facility is to determine the fundamental and interactive radiation-response phenomena for candidate structural materials at high fluence. An appropriate combination of tests in the fusion facility with tests in large-volume, high-fluence fission reactors can then be used to predict fusion-component lifetime. The reliability of these predictions can be increased by incorporating interactive simulation tests in the fusion-materials test facility. Moreover, accel-

erated testing is required in order to provide the necessary design data in a timely manner.

In addition to physical and mechanical property tests, specific tests must be designed for interactive failure mechanisms. Examples are swelling/creep interactive tests in uniaxial and multiaxial stress state, creep/fatigue interactive tests, and radiation-hardening/deformation tests. Sizes and geometries must be chosen to reveal the failure modes and fluence for the onset of failure. Useful design information for FW/B interactive tests can be achieved if the following requirements are satisfied in the fusion-materials test facility:

(1) displacement damage dose: ~ 50 – 200 dpa, (2) test volume: ~ 100 – 1000 cm³, (3) test temperature: \sim R.T. to 1000°C , (4) test configuration: disks, tension specimens, tubes, and fracture toughness specimens, (5) cycling frequency: ≥ 100 Hz, (6) *in situ* diagnostics: temperature, strain, pressure, and radiation dosimetry, and (7) damage parameters: $\geq 80\%$ of neutrons have 14-MeV energy, He/dpa ≈ 10 – 100 .

3. TESTING REQUIREMENTS FOR HIGH-HEAT-FLUX COMPONENTS

High-heat-flux components are currently tested in a series of laboratory devices capable of reproducing certain features of the plasma edge. The devices include electron- and ion-beam sources to deliver intense surface heat loads, and small plasma devices to expose the materials to plasma erosion and to study hydrogen isotope behavior. These facilities, in conjunction with postmortem evaluations of hardware from operational tokamaks, have been successful in identifying key issues and in assisting the development of optimum HHF components for current generation machines. For neutron-producing devices, the problem of defining relevant materials and component tests becomes much more difficult. What is actually required is a test facility that is capable of exposing test hardware to an operational neutron-flux level while simultaneously generating the proper temperature gradients. This is necessary because the neutron exposure will occur while the component is exposed to the surface heat flux, thus having a large temperature gradient through the material. When the pulse is over, the stresses that are generated on cooling may be more severe than the "on level" stresses. Any isothermal neutron exposure will not fully explore this issue.

In general, the neutron effects that are expected to have the largest impact on HHF component operation are reductions in thermal conductivity and changes in mechanical properties that will lead to a reduction in thermal shock resistance.⁽²⁴⁾ Graphite, for instance, will suffer reductions in these properties which will limit the thickness that can be used and, as a result, shorten the expected lifetime. Other concerns are neutron-irradiation-induced density changes (densification and swelling), differential swelling between the armor and the substrate materials, degradation of interfaces, radiation-induced modifications in the material's microstructure (precipitate dissolution or coarsening), and changes in mechanical properties induced by transmutation products, e.g., helium, hydrogen, etc. The stress state generated in the component will be modified by radiation-enhanced creep, which relieves operational stresses, but possibly generates large residual stresses while the machine is off.

An example of a thermal-stress-generated failure is shown in Fig. 10. This tile was fabricated by brazing an isotropic graphite armor tile to a water-cooled inconel substrate. The brazing of a low expansion graphite to a higher expansion inconel substrate results in the generation of large residual stresses in the component as it cools from the brazing temperature (in this case 870°C) to room temperature. Hence, at room temperature, the graphite has a large residual compressive stress. Then, when the tile was exposed to a surface heat flux of 5 MW/m², additional compressive forces were generated by the temperature gradients. This led to graphite fracture which resulted in component failure about 4 seconds into the pulse. This dramatic example of thermal-stress-generated failure in an unirradiated component demonstrates the severity of this environment and the importance of a suitable test facility to identify lifetimes and operational limits, and to optimize the HHF component design prior to construction.

At the current time, the only methods by which neutron irradiation effects can be studied is by fabricating small test coupons of candidate materials, exposing them to a neutron fluence in fission reactors, and then evaluating their responses using facilities like those mentioned previously. Some materials such as graphite or beryllium do not activate significantly and can be tested in existing facilities, e.g., thermal shock tests on neutron-irradiated graphite will be carried out using an existing electron beam test system. However, samples that are brazed or that contain copper or most other metals will become

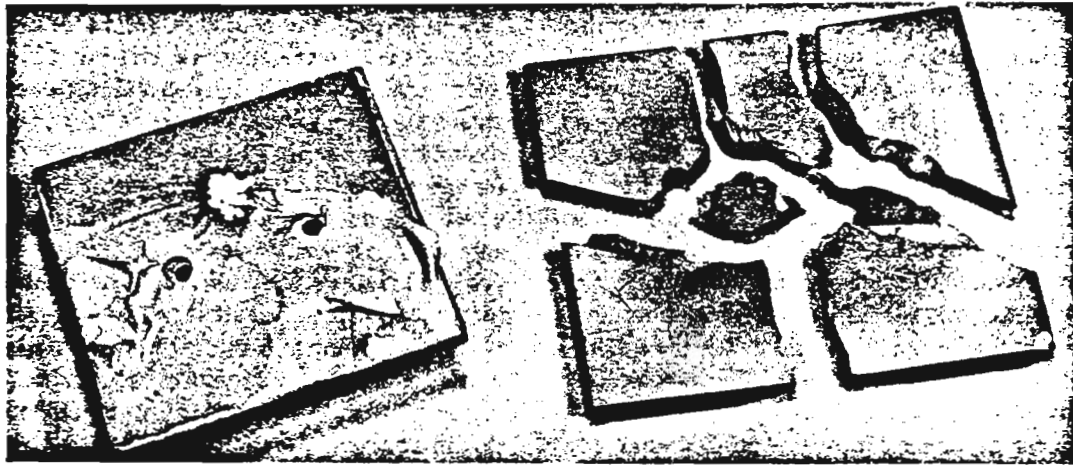


Fig. 10. Example of thermal-stress-generated failure.

highly radioactive after exposure and must be tested in appropriate hot cell facilities. Sandia National Laboratories is currently constructing an electron-beam test system for a hot cell so that these tests can be performed. Although these tests will give some initial indication of the issues involved, they have several drawbacks. They will not test 14-MeV neutron effects, e.g., the correct helium generation rate, etc., exposure with the proper temperature and stress gradients, or a pulsed exposure.

In summary, the basic types of test configurations which are possible for HHF components are shown in Table I. Although the type III tests which are currently under way are supplying some information, it will be necessary to move to a type I or II test facility if HHF components are to be designed for future devices with a high degree of confidence.

4. CONCLUSIONS

We conclude that a dedicated fusion-materials test facility is a cornerstone in an overall materials-development strategy. Without this facility, design qualifications of structural and HHF components will be uncertain. We have illustrated here that the interactive effects of radiation lead to failure modes which cannot be anticipated from our knowledge of fundamental radiation-response phenomena alone. It is necessary, therefore, to develop a facility where tests for the interactive effects of radiation can be performed. For this facility to meet the goal of producing useful design data, it must meet minimal operational requirements. (1) A large fraction of neutrons must have energy around 14 MeV in order to provide the correct damage parameters which are

Table I. Basic Types of Test Configurations for High-Heat-Flux Components

	Type I: most relevant ^a	Type II: acceptable ^b	Type III: some information ^c
Spectrum	14 MeV	14 MeV	Fission
Surface heat	<i>In situ</i>	Separate	Separate
Sample size	> 10 cm ³	> 2 cm ³	> 2 cm ²
Total sample volume	> 20 cm ³	> 10 cm ³	> 10 cm ³
Cycles	> 10 ³	> 10 ⁴	> 10 ⁴
Active cooling required	Yes	No	No
<i>In situ</i> diagnostics	Temperature, visual, strain	Temperature	Temperature

^a14-MeV source, *in situ* heating by plasma or electron beams.

^b14-MeV source, isothermal; testing external.

^cFission source, isothermal; testing external.

relevant to fusion components. (2) Tests must be accelerated so that meaningful results can be obtained in a reasonably short time. (3) A high pulsing frequency, i.e., $\geq \sim 100$ Hz, or steady-state operation is necessary to eliminate the effects of pulsed radiation. (4) Means of controlling the temperature (25° – 1000° C) and the temperature gradient across the surface of components should be provided. The proper temperature gradient is particularly important for duplex, bonded, HHH components. (5) The required displacement-damage dose for many failure mechanisms is high, and the facility must be able to deliver a displacement-damage dose of ~ 50 – 200 dpa at a duty factor ≥ 0.8 . (6) The required prime test volume will depend on the number and type of tests, and on future developments in miniature sample and component technology. It may be possible to develop special tests for interactive failure mechanisms which simulate the effects of temperature, temperature gradients, geometry, and external constraints in the fusion environment. A test volume of 100 – 1000 cm³ may be necessary for these interactive tests. (7) *In situ* diagnostics and control will be required for measurements of temperature, strain, pressure, and radiation dosimetry.

ACKNOWLEDGMENTS

This work was supported by the U.S. Department of Energy, Office of Fusion Energy, Grant No. DE-FG03-84ER52110, with UCLA. Permission of J. P. Blanchard to use some of his joint work with N. M. Ghoniem is acknowledged.

REFERENCES

1. D. L. Smith (1981). *J. Nucl. Mater.*, **103/104**, 19.
2. R. E. Nygren (1981). *J. Nucl. Mater.*, **103/104**, 31.
3. R. Behrisch (1979). *J. Nucl. Mater.*, **85/86**, 1047.
4. R. F. Mattas, D. L. Smith, and M. A. Abdou (1984). *J. Nucl. Mater.*, **122/123**, 66.
5. M. C. Carroll (1986). *Technical Assessment of Plasma-Interactive Options for Claddings and Attachments for Steady State* (University of California Los Angeles Report No. UCLA-ENG-8726/PPG-1085).
6. R. W. Conn (1981). *J. Nucl. Mater.*, **103/104**, 7.
7. W. B. Gauster, J. A. Koski, and R. D. Watson (1984). *J. Nucl. Mater.*, **122/123**, 80.
8. J. B. Whitley (1985). *J. Nucl. Mater.*, **133/134**, 39.
9. R. C. Isler (1984). *Nucl. Fusion*, **24**, 1599.
10. S. Ishino, P. Shiller, and A. Rowcliffe (1989). *J. Fusion Energy*, **8**(3), 147.
11. G. L. Kulcinski, R. Lott, P. Singer, and D. Brown (1974). *Nucl. Technol.*, **22**, 20.
12. A. D. Adegbulugbe and J. E. Meyer (1981). *J. Nucl. Mater.*, **103/104**, 161.
13. S. D. Harkness and B. A. Cramer (1979). *J. Nucl. Mater.*, **85/86**, 135.
14. J. R. Power and M. Reich (1980). *Nucl. Engr. Des.*, **58**, 247.
15. M. J. Delaney, B. A. Cramer, and C. A. Trachsel (1979). *J. Nucl. Mater.*, **85/86**, 165.
16. W. Daenner and J. Raeder (1979). *J. Nucl. Mater.*, **85/86**, 147.
17. W. Daenner and J. Raeder (1981). *J. Nucl. Mater.*, **103/104**, 121.
18. R. D. Watson (1981). *The Impact of Inelastic Deformation Radiation Effects and Fatigue Damage on Fusion Reactor First Wall Lifetime*, Ph.D. thesis (University of Wisconsin, Madison) December 1981.
19. R. F. Mattas (1980). *Fusion Component Lifetime Analysis* (Argonne National Laboratory Report No. ANL/FPP/TF-160).
20. B. G. Logan et al. (1983). *Mirror Advanced Reactor Study Interim Design Report* (Lawrence Livermore National Laboratory Report No. UCRL-5333).
21. *The Titan Reversed-Field Pinch Fusion Reactor Study. Final Report* (1989). (University of California Los Angeles Report No. UCLA-PPG-1200).
22. R. J. Amodeo and N. M. Ghoniem (1985). *Nucl. Engr. Des./Fusion*, **2**, 97.
23. J. P. Blanchard and N. M. Ghoniem (1984). *J. Nucl. Mater.*, **122**(2), 101.
24. M. F. Smith and J. B. Whitley (1986). In *Physics of Plasma-Wall Interactions in Controlled Fusion*, D. E. Post and R. Behrisch, eds. NATO ASI series, series B, Physics: V. 131 (Plenum Press, New York), pp. 539-605.